MODERN ASPECTS OF PHYSICAL CHEMISTRY OF IONIC SOLUTIONS *

Josef Barthel
Institute of Physical and Theoretical Chemistry
University of Regensburg, Germany

Summary

Modern theory of ionic solutions depends upon information on a variety of experimental methods for a realistic adjustment of parameters. Hamiltonian models yield reliable equations for various solution properties with a unique set of basic parameters resulting from fits of different appropriate experiments, thus permitting the simulation of the properties of other electrolyte solutions for which data are not available. In this way knowledge-based data bases provide the property profiles of electrolyte solutions for applied research and technology.

A survey is given of the information on structure and dynamics of electrolyte solutions obtained from high frequency permittivity measurements and of chemical models at McMillan-Mayer level permitting the calculation of electrolyte solution properties. The interplay of thermodynamic, transport, spectroscopic, kinetic and computer simulation methods is stressed. Illustrative examples are quoted.

1.   Introduction

The progress in electrochemical technology during the last decade displays the role of electrolyte solutions in applied science and chemical engineering. A large variety of solvents, solvent mixtures and more or less complex ionic compounds gained the interest of scientists all over the world, documented by an increasing number of publications. The electolyte data base ELDAR [1 to 3] shows an input of more than 2.000 papers per year with about 50.000 data tupels on thermodynamic, transport, dielectric, spectroscopic and kinetic data of electrolyte solutions, not included the contributions about electrode processes. The high flexibility of electrolyte solutions for tackling technical problems, evidenced by their wide variety of suitable solvents with widely spread physical properties such as viscosity, permittivity, freezing and boiling point, vapor pressure, stability or solvation power, and an almost unlimited scale of properties offered by the mixed solvent systems permits the realization of electrolyte solutions with properties planned on the drawing board [4].

The actual paper gives a survey on some modern developments in solution chemistry which may be helpful to practizing electrochemists for the modern understanding of electrolyte solutions.It would like to be a guide in their choice for tackling problems.

---

2. Information on Structure and Dynamics of Electrolyte Solutions from Dielectric Relaxation Measurements

2.1 Theoretical background

A homogeneous system of dipole molecules representing the solvent of an electrolyte solution, placed in an electric field $\vec{E}$ answers by its equilibrium polarization

$$\vec{P} = \varepsilon_o(\varepsilon_s - 1)\vec{E} \tag{1}$$

ε_o is the permittivity of the vacuum, ε_s is the static relative permittivity. The electric polarization $\vec{P}$ consists of two parts: the orientational polarization $\langle\vec{P}_\mu\rangle$ resulting from the alignment of the permanent dipole moments $\vec{\mu}_i$ in the electric field against thermal motion, $\langle\vec{P}_\mu\rangle = \langle\sum\vec{\mu}_i\rangle$, and the induced polarization $\langle\vec{P}_\alpha\rangle$ stemming from the induction of dipole moments $\vec{\mu}_i^{ind} = \alpha_i\vec{E}$ induced by the external field at the position of particle i, $\langle\vec{P}_\alpha\rangle = \langle\sum\vec{\mu}_i^{ind}\rangle$; α_i is the polarizability of the dipole molecule. $\vec{P}_\mu$ and $\vec{P}_\alpha$ are considered to be linearly independent.

$$\langle\vec{P}\rangle = \langle\vec{P}_\mu\rangle + \langle\vec{P}_\alpha\rangle; \quad \langle\vec{P}_\mu\rangle = \varepsilon_o(\varepsilon_s - \varepsilon_\infty)\vec{E}; \quad \langle\vec{P}_\alpha\rangle = \varepsilon_o(\varepsilon_\infty - 1)\vec{E} \tag{2a,b,c}$$

The separation of $\langle\vec{P}_\mu\rangle$ and $\langle\vec{P}_\alpha\rangle$ is possible with the help of frequency-domain measurements. $\langle\vec{P}_\mu\rangle$ and $\langle\vec{P}_\alpha\rangle$ are frequency-independent quantities at frequencies ν (circular frequency $\omega = 2\pi\nu$) up to some hundred MHz, where the dipole-moment orientation follows the polarity changes of the external electric field without time lag. $\langle\vec{P}_\mu\rangle$ decreases when the polarity changes of the alternating field cause significant variation of the electric field strength within periods that are characteristic of molecular motions changing $\sum\vec{\mu}_i$, such as dipole orientation, mobility, or chemical reactions and H-bonding. For the liquids generally used as the solvents of electrolyte solutions the permittivity decrease occurs at HF/MW frequencies; $\langle\vec{P}_\mu\rangle$ reaches zero in the FIR/IR region where the permittivity is ε_∞. At these frequencies $\langle\vec{P}_\alpha\rangle$ is still unaffected as an intramolecular effect. $\langle\vec{P}_\alpha\rangle$ decreases at very high frequencies as a consequence of atomic and electron resonance effects.

On the other hand, when in a time domain experiment a static field $\vec{E}(\nu = 0)$ initially applied to the system of molecular dipoles, is switched off at time t = 0, $\langle\vec{P}_\alpha\rangle$ breaks down without time lag, whereas $\langle\vec{P}_\mu\rangle$ decreases monotonically with time to its final value $\langle\vec{P}_\mu\rangle = 0$.

$$\langle\vec{P}_\mu(0)\vec{P}_\mu(t)\rangle = \langle\vec{P}_\mu(0)\vec{P}_\mu(0)\rangle F_p^{or}(t); \quad F_p^{or} = \frac{\langle\vec{P}_\mu(0)\vec{P}_\mu(t)\rangle}{\langle\vec{P}_\mu(0)\vec{P}_\mu(0)\rangle} \tag{3a,b}$$

The step-response function of the orientational polarization $F_p^{or}(t)$ is of the relaxational type defining the relaxation time τ of the process.

It must be stressed that step-response functions F_p^{or} are macroscopic (phase) properties. To obtain information on the molecular level they must be converted into molecular autocorrelation functions $\phi(t)$ defining the molecular relaxation times τ'

$$\phi(t) = \langle\cos\Theta\rangle = \frac{\langle\vec{\mu}(0)\vec{\mu}(t)\rangle}{\langle\vec{\mu}(0)\vec{\mu}(0)\rangle} \tag{4}$$

The proper conversion of $F_p^{or}(t)$ into $\phi(t)$ is still a matter of discussion. In cases where the rotation of the dipole molecule can be described by a rotational diffusion model, macroscopic (τ) and microscopic (τ') relaxation times may be approximately related by the Powles-Glarum equation [5]

$$\tau' = \frac{2\varepsilon_s + \varepsilon_\infty}{3\varepsilon_s}\tau \tag{5}$$

and τ' is proportinal to the molecular size of the rotating dipole molecule and the solvent viscosity η [6]

$$\tau' = \frac{3V_m\eta}{kT}fC \tag{6}$$

In eq. (6) V_m is the molecular volume, f is a factor depending on the molecular shape, and C is a factor coupling microscopic and macroscopic viscosity.

The time-dependent response of polarization $\langle\vec{P}_\mu(t)\rangle$ to an arbitrarily changing electric field $\vec{E}(t)$ can be approximated by splitting up the field into a number of Δt block functions where $E(t')$ is the field strength for the interval $t' \le t \le t' + dt'$ yielding [7]

$$\langle\vec{P}_\mu(t)\rangle = \varepsilon_o(\varepsilon_s - \varepsilon_\infty)\int_{-\infty}^{t}\vec{E}(t - t')f_p^{or}(t')dt'; \quad f_p^{or}(t') = -\frac{\partial F_p^{or}(t')}{\partial t'} \tag{7a,b}$$

$f_p^{or}(t')$ is called pulse-response function.

Frequency domain experiments are carried out at a series of increasing frequencies of harmonically changing monochromatic electromagnetic waves, $\vec{E}(t) = \vec{E}_o\exp(i\omega t)$, yielding the time dependence of polarization in an electromagnetic field of circular frequency ω

$$\langle\vec{P}_\mu(\omega, t)\rangle = \varepsilon_o(\varepsilon_s - \varepsilon_\infty)\vec{E}(t)\int_0^\infty e^{-i\omega t'}f_p^{or}(t')dt' \tag{8}$$

$$= \varepsilon_o(\varepsilon_s - \varepsilon_\infty)\vec{E}(t)\mathcal{L}_{i\omega}^o[f_p^{or}(t')]$$

where $\mathcal{L}_{i\omega}[f_p^{or}(t')]$ is the Laplace transform of the pulse-response function. Eq. (8) shows that $\vec{P}_\mu(\omega, t)$ is a complex quantity as a consequence of the complex quantity $\vec{E}_o\exp(i\omega t)$. The combination of eq. (8) and eq. (1) where $\vec{P}_\mu$ and consequently ε are written as complex quantities leads to the frequency-dependent complex permittivity

$$\hat{\varepsilon}(\omega) = \varepsilon'(\omega) - i\varepsilon''(\omega) = (\varepsilon_s - \varepsilon_\infty)\mathcal{L}_{i\omega}^o[f_p^{or}(t')] \tag{9}$$

with a real part $\varepsilon'(\omega)$ reproducing the dispersion of permittivity and an imaginary part $\varepsilon''(\omega)$ reproducing absorption. The energy dissipated in the sample per unit of volume and time is

$$\dot{W} = \frac{1}{2}E_o^2\omega\varepsilon_o\varepsilon''(\omega) \tag{10}$$

The information on structure and dynamics of dipolar liquids is hidden in the step-response function F_p^{or} or pulse-response function f_p^{or}. The characteristic times of

molecular motions which change the mean dipole moment $\langle \sum \vec{\mu}_i \rangle$ are determined in time-domain and frequency -domain measurements as the relaxation times τ_j of the molecular processes. A simple case is chosen to illustrate the relation of the response functions F_p^{or} and f_p^{or} and the underlying relaxation time. It is assumed that only one dipolar reorientation time τ is responsible for the change of $\langle \vec{P}_\mu \rangle$ and that molecular reorientation is a first order process of rate constant $k = \tau^{-1}$

$$\frac{d\langle \vec{P}_\mu(0)\vec{P}_\mu(t)\rangle}{dt} = k\langle \vec{P}_\mu(0)\vec{P}_\mu(t)\rangle; \quad \langle \vec{P}_\mu(0)\vec{P}_\mu(t)\rangle = \langle \vec{P}_\mu(0)\vec{P}_\mu(0)\rangle \exp(-\frac{t}{\tau}) \quad (11a,b)$$

Then

$$F_p^{or}(t) = \exp(-\frac{t}{\tau}); \quad f_p^{or} = \frac{1}{\tau}\exp(-\frac{t}{\tau}) \quad (12a,b)$$

yield the frequency dependence of permittivity according to eq. (9)

$$\hat{\varepsilon}(\omega) = \varepsilon_\infty + \frac{\varepsilon_s - \varepsilon_\infty}{1 + i\omega\tau}; \quad \varepsilon'(\omega) = \varepsilon_\infty + \frac{\varepsilon_s - \varepsilon_\infty}{1 + \omega^2\tau^2}; \quad \varepsilon''(\omega) = \frac{(\varepsilon_s - \varepsilon_\infty)\omega\tau}{1 + \omega^2\tau^2} \quad (13a,b,c)$$

In our laboratory the dispersion and absorption curves $\varepsilon'(\omega)$ and $\varepsilon''(\omega)$ are determined in the frequency range from 1 - 100 GHz by a method of travelling waves with the help of attenuation and phase shift measurements. The propagation coefficient $\hat{k}$ of the elctromagnetic wave in an electrically non-conducting liquid follows from the Maxwell equations as

$$\hat{k} = k_o\hat{\varepsilon}(\omega); \quad k_o = \frac{\omega}{c} \quad (14a,b)$$

where c is the speed of light and k_o is the propagation coefficient of the electromagnetic wave in the vacuum.

The application of electromagnetic waves to electrolyte solutions changes the preceding theoretical considerations in only one point. The freely moving charges in electrolyte solutions produce electric conductance. According to Maxwell moving charges contribute to the propagation coefficient $\hat{k}$

$$\hat{k} = k_o[\hat{\varepsilon}(\omega) + \frac{\hat{\sigma}(\omega)}{i\omega\varepsilon_o}] \quad (15)$$

In eq.(15) $\hat{\sigma}(\omega)$ is the frequency dependent specific conductivity of the solution. This consequence of the Maxwell equations shows that permittivity and specific conductivity of electrolyte solutions cannot be measured separately. The appropriate material constant for electrolyte solutions is the 'generalized' permittivity $\hat{\eta}(\omega)$

$$\hat{\eta}(\omega) = \hat{\varepsilon}(\omega) + \frac{\hat{\sigma}(\omega)}{i\omega\varepsilon_o}; \quad \eta'(\omega) = \varepsilon'(\omega) - \frac{\sigma''(\omega)}{\omega\varepsilon_o}; \quad \eta''(\omega) = \varepsilon''(\omega) + \frac{\sigma'(\omega)}{\omega\varepsilon_o} \quad (16a,b,c)$$

where

$$\lim_{\omega \to 0} \hat{\sigma}(\omega) = \sigma'(0) = \sigma; \quad \sigma''(0) = 0 \quad (17a,b)$$

The specific conductivity σ of the solution at low frequencies is measurable by classical methods (Kohlrausch bridge and conductance cell)

$$\sigma = e\sum \rho_k|z_k|u_k; \quad \lambda_k = eN_Au_k \quad (18a,b)$$

In eqs. (18) ρ_k, z_k and λ_k are the particle density, valency and conductance of the ion k; u_k is the ionic mobility, $u_k = e|z_k|\zeta_k^{-1}$; ζ_k is the friction factor of the moving ion k in the solution; N_A is Avogadro's number and e is the elementary charge. The frequency dependence of conductivity is very small (Debye-Falkenhagen effect) and can be neglected at high frequencies: $\sigma''(\omega)/\omega\varepsilon_o \approx 0$ [8]. The eqs. (16b,c) can be reduced to

$$\eta'(\omega) = \varepsilon'(\omega); \quad \eta''(\omega) = \varepsilon''(\omega) + \frac{\sigma}{\omega\varepsilon_o} \quad (19a,b)$$

2.2 Polar liquids

Fig. 1 shows the dispersion curve $\varepsilon'(\omega)$ according to eq. (13b), the absorption curve $\varepsilon''(\omega)$ according to eq. (13c) and the Argand diagram (Cole-Cole plot) ε'' vs. ε' for water at 25 ° C obtained from measurements at 1.8 to 100 GHz [9]. The Argand diagram is a semicircle

$$[\varepsilon'(\omega) - \frac{\varepsilon_s + \varepsilon_\infty}{2}]^2 + [\varepsilon''(\omega)]^2 = [\frac{\varepsilon_s - \varepsilon_\infty}{2}]^2 \quad (20)$$
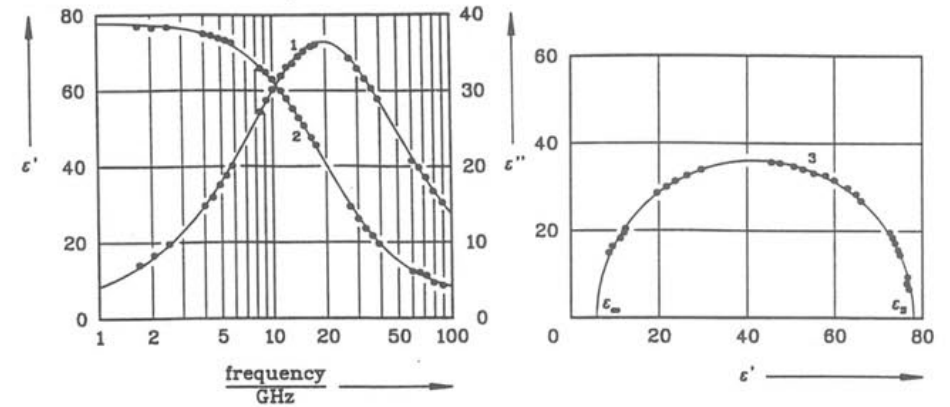
Fig. 1: Dispersion curve (1), absorption curve (2) and Argand diagram (3) of water at 25° C in the frequency range 1.8 to 100 GHz.

Figs. 1 impart the following information : $\varepsilon_s = \varepsilon'(0) = 78.4$, $\varepsilon_\infty = \varepsilon'(\infty) = 5.2$ and $\tau = 8.3\,ps$. The relaxation time τ is the reciprocal value of the frequency at the maximum of $\varepsilon''(\omega)$, at the inflection point of $\varepsilon'(\omega)$, or at the apex of the Argand diagram, $\tau = \omega_{max}^{-1}$.

It must be stressed that the information from figs. 1 is an incomplete information on the dynamic processes in water and only an approximative information on the considered particular molecular reorientation process. The use of Laplace integrals in eq. (8), extended from zero to infinity, would require the knowledge of all relaxation modes of the liquid or, at least, measurements in a sufficiently wide frequency range

to permit extrapolation to these limits. For the problem of incomplete frequency coverage the reader is referred to ref. [10]. However, precise measurements in restricted frequency ranges may yield satisfacotry information on processes taking place at these frequencies. For instance, the extension of measurements on water to 1 - 400 GHz does not change the relaxation time of the reorientation time $\tau = \tau_1 = 8.3ps$, but a second relaxation time τ_2 is observed at 1 ps due to H-bonding; ε_s is slightly changed and ε_∞ is significantly decreased, as could be expected since every new process at high frequencies must decrease ε_∞ until its value at IR frequencies ($\varepsilon_\infty = 1.8$) is reached. This example shows that further dissipative processes at high frequencies must be expected for water.

The results from measurements of our laboratory on various polar liquids at frequencies from 1 to 90 GHz and the discussion of the underlying molecular modes were published recently [11] [12]. A table containing also literature data is given in ref. [13].

The occurrence of more than one relaxation time in liquids can be analyzed with pulse-response functions of the type [7]

$$f_p^{or} = \sum_{j=1}^{n} \frac{g_i}{\tau_j} \exp(-\frac{t}{\tau_j}) \quad or \quad f_p^{or} = \int_0^\infty \frac{g(\tau)}{\tau} \exp(-\frac{t}{\tau}) d\tau \qquad (21a,b)$$

for discrete or continuous distributions of relaxation times, respectively. Only discrete relaxation time distributions will be considered in following discussions yielding the frequency dependence of permittivity when N relaxation processes take place

$$\hat{\varepsilon}(\omega) = \varepsilon_\infty + (\varepsilon_s - \varepsilon_\infty) \sum_{j=1}^{N} \frac{g_j}{1 + i\omega\tau_j} ; \quad g_j = \frac{\varepsilon_j - \varepsilon_{\infty j}}{\varepsilon_s - \varepsilon_\infty} ; \quad \varepsilon_{j\infty} = \varepsilon_{j+1} \qquad (22a,b,c)$$

Eqs. (22) produce Argand diagrams with a sequence of semicircles of dispersion amplitude $(\varepsilon_j - \varepsilon_{\infty j})$; examples are given in figs. 3.

For non-hydrogen bonding systems the reorientation of single molecules is responsible for the slow relaxation process [12]; the corresponding dispersion amplitude $(\varepsilon_j - \varepsilon_{j\infty})$ is proportional to the particle density ρ of the relaxing species [14]

$$\varepsilon_i - \varepsilon_{i\infty} = \frac{\rho}{3kT\varepsilon_o} \frac{3\varepsilon_j}{2\varepsilon_j + 1} \frac{g\mu^2}{(1 - f\alpha)^2} \qquad (23)$$

Eq. (23) results from the Kirkwood-Onsager theory of static polarization; g is the Kirkwood correlation factor; f is the reaction field factor of the Onsager theory. Additional high frequency processes may arise from intramolecular reorientation [12].

Liquids exhibiting cooperative effects such as hydrogene bonding show rather complex dielectric behavior. Water with two relaxation times was given as an example for a liquid producing a three dimensional network. Alcohols producing one-dimensional association show three relaxation times [15][11] and so does N-methylformamide [12].

Mixtures of polar compounds produce Argand diagrams with semicircles attributable to their compounds. The variation of dispersion amplitudes and relaxation times of the individual relaxation regions with mole fraction are characteristic for molecular interactions. Apolar compounds cannot undergo relaxation processes for lack of orientable dipoles. In mixtures with polar compounds they diminish the dispersion amplitudes of the polar compounds by a volume effect. Examples can be found in refs. [9] [16 to 22].

Modern kinetic theories use 'longitudinal relaxation rates' $\tau_L = \varepsilon_\infty \tau / \varepsilon_s$ [23][24] derived from solvent relaxation times τ for the calculation of rate constants of fast chemical reactions such as electron transfer reactions in solutions [25 to 28].

The role of solvent relaxation times for transport properties will be discussed in the following chapter.

2.3   Electrolyte solutions

The permittivity diagrams of electrolyte solutions differ from those of polar compounds by the contribution of specific conductivity σ to the generalized permittivity. However, the measured $\eta'(\omega)$ and $\eta''(\omega)$ graphs can easily be reduced to $\varepsilon'(\omega)$ and $\varepsilon''(\omega)$ diagrams when they are corrected for the conductance contribution according to eqs. (19). Dispersion, absorption and Argand diagrams as obtained after conductance correction will be the subject of the following discussion. For diagrams without conductance correction and their discussion, see refs. [10] [29] [30].

2.3.1   Dielectric depression by ions

Freely moving ions without dipole moments in solutions cannot be orientated in electric fields. Therefore they cannot produce orientational relaxation times. However, ions change the local electric field acting on the adjacent solvent molecules and diminish the solvent dispersion amplitude significantly stronger than the volume effect of hard spheres predicts. The static permittivity $\varepsilon_s(c)$ of the solvent at electrolyte concentration c characteristically decreases with ion size and charge. For diagrams of $\Delta\varepsilon$ vs. c and the discussion of ion specificity of the dielectric depression $\Delta\varepsilon, \Delta\varepsilon = \varepsilon_s(0) - \varepsilon_s(c)$, see refs. [10] [29] [31]. Dielectric depression is commonly presented by the relation

$$\Delta\varepsilon = \delta_\varepsilon \cdot c - \beta_\varepsilon c^n \quad (n = 3/2 \, or \, 2) \qquad (24)$$

The dielectric decrement δ_ε and the coefficient β_ε for various electrolyte solutions is tabulated in ref. [13].

The dielectric depression $\Delta\varepsilon$ at electrolyte concentration c, eq. (24), consists of three parts

$$\Delta\varepsilon = \Delta\varepsilon_{col} + \Delta\varepsilon_{solv} + \Delta\varepsilon_{kin} \qquad (25)$$

where $\Delta\varepsilon_{vol}$ is the volume effect which also would be observed when apolar particles of equal size are dissolved; $\Delta\varepsilon_{solv}$ is the already mentioned additional effect due to irrotationally bounding of solvent molecules in solvation shells, due to ion-solvent molecule interaction; $\Delta\varepsilon_{kin}$ is a kinetic depolarization effect, reducing the mobility of the moving ions. The subdivison into partial effects is also possible for the dielectric decrement δ_ε and the coefficient β_ε.

Thermodynamic solvation models estimate the number of irrotationally bound solvent molecules. Pottel et al. [32 to 34], estimate 'effective' volume fractions of the solvent and compare them to 'analytical ' volume fractions to obtain solvation numbers. Lestrade et al. [35] [36] use the Kirkwood-Fröhlich equation to relate the calculated dielectric decrement δ_ε to its measured value. A critical discussion of Pottel's and Lestrade's solvation numbers is given in ref. [31].

Conductance theory defines ionic mobilities u_i with the help of friction coefficients ζ_i, see eq.(18). Ion solvation causes an increase of the radius of the moving ion which can be taken into account when expressing the *mechanical* friction coefficient according to Stokes' law with the help of an 'effective' particle radius

$$\zeta_{st} = y\eta R_{eff} \qquad (26)$$

η is the viscosity of the solvent in which the spherical particle of radius R_{eff} moves under slip $(y = 4\pi)$ or stick $(y = 6\pi)$ conditions. According to Hubbard and Onsager [37] [38] the mutual interaction due to the dielectric properties of the solvent and ionic mobility is taken into account by an additional *dielectric* friction coefficient

$$\zeta_{HO} = \eta R_{HO}\sum a_j\left(\frac{R_{HO}}{R_{eff}}\right)^j; \quad R_{HO} = [\frac{z^2 e^2\tau(0)}{64\pi^2\eta\varepsilon_o\varepsilon^2(0)}(\varepsilon(0)-\varepsilon_\infty(0))]^{1/4} \quad (27a,b)$$

The coefficients a_j of the series development are given in ref. [39]. Extensions of eqs. (27) to the case of solvents with more than one relaxation process and to the case of mixed solvents as well as a critical examination of the theory are given by Ibuki and Nakahara [40] and Kessler [41].

According to the continuum theory of Hubbard and Onsager [37] kinetic polarization $\Delta\varepsilon_{kin}$ results from ion migration in an external field $\vec{E}$ by diminution of the orientational polarization of the solvent; $\Delta\varepsilon_{kin}$ is proportional to specific conductivity σ and a factor depending on the dielectric data $\varepsilon_s(0), \varepsilon_\infty(0)$ and $\tau(0)$ of the pure solvent

$$\Delta\varepsilon_{kin} = p\frac{\varepsilon_s(0)-\varepsilon_\infty(0)}{\varepsilon_o\varepsilon_s(0)}\tau(0)\sigma \qquad (28)$$

$p = 2/3$ under slip and $p = 1$ under stick conditions. Improvements of the theory are due to Felderhoff [42]; a molecular theory was developed by Hubbard, Colonomos and Wolynes [43].

The linear relation $\Delta\varepsilon$ vs. σ is found in many cases; however, the experimental slope does not correspond to the theoretically predicted one due to the incomplete account of $\Delta\varepsilon_{solv}$ and the neglection of $\Delta\varepsilon_{vol}$. The ad hoc combination of 'irrotationally bound' solvent molecules and continuum theory of $\Delta\varepsilon_{kin}$ permits to bring

experimental and theoretical slope to coincidence when solvation numbers are used for adaptation, see fig. 2. For further examples, see refs. [30][31][44].
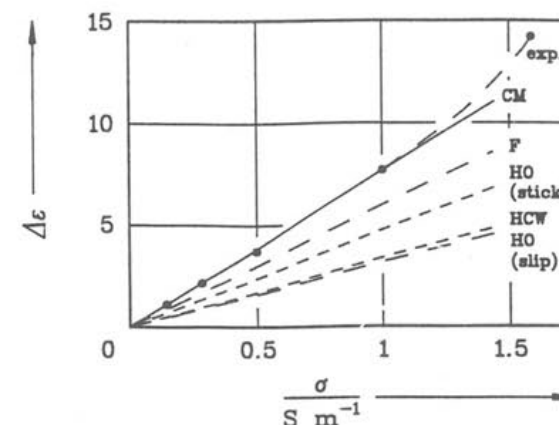
Fig. 2: Theories of kinetic depolarization [74]
full points: experimental data Bu$_4$NCl/CH$_3$OH (25° C); HO: Hubbard-Onsager; HCW: Hubbard, Colonomos, Wolynes; F: Felderhoff; full line: combination of kinetic depolarization and solvation model (10 solvent molecules irrotationally bound in solvation shells).

2.3.2 Influence of ion charges on solvent relaxation times

The dependence of solvent relaxation times on electrolyte concentration reveals characteristic differences between hydrogen bonding and dipolar aprotic solvents, cf. ref. [10]. The main (low) relaxation time of dipolar aprotic solvents increases monotonically with increasing viscosity at increasing electrolyte concentration, as expected from eq. (6). In contrast, the main relaxation time of hydrogen-bonding liquids is intimately linked to the structure of the solvent and the nature of solute. For instance, the addition of an electrolyte to N-methylformamide may cause a monotonously decreasing relaxation time whereas the relaxation time of methanol increases slightly and goes through a maximum at increasing salt concentration. In H-bonding solvents the long range order through winding hydrogen-bonding chains is broken up in the amide, whereas in the alcohol the bulk structure is relatively unaffected or even stabilized at low electrolyte concentrations. The fast relaxation process in hydrogen-bonding liquids attributed to the dynamics of the hydrogen bond is independent of the concentration and nature of all dissolved electrolytes studied so far.

2.3.3 Ion aggregate formation in electrolyte solutions

Since Bjerrum's pioneering work on the concept of ion-pair formation this problem has been extensively studied in the literature. Chemists discuss ion pairs of various type in electrolyte solutions, theoreticians accept ion-pair formation as a possibility

for the formulation of short-range interactions although they do not need the ion-pair concept in their ion-ion correlation functions.

The chemical model of electrolyte solutions assumes ion-pair formation in solutions when after dissolution of an ionophore as solvated ions in a first step, cations C^{z+} and anions A^{z-} form paired states of oppositely charged ions

$$C_{\nu_+}^{z+} A_{\nu_-}^{z-} \to \nu_+ C^{z+} + \nu_- A^{z-} \underset{k_2}{\overset{k_1}{\rightleftharpoons}} [C_{\omega+}^{z+} A_{\omega-}^{z-}]; \quad K_{ass} = \frac{k_1}{k_2} \quad (29a,b)$$

The ion pair can be a neutral ($\omega_+ = \omega_-$) or charged ($\omega_+ \neq \omega_-$) species. k_1 and k_2 are the rate constants of ion-pair formation and decomposition; K_{ass} is the association constant. A symmetrical electrolyte ($\nu_+ = \nu_- = 1; z_+ = |z_-|$) produces only neutral ion pairs with or without inclusion of solvent molecules yielding contact ion pairs $[C^{z+} A^{z-}]^o$ and solvent separated ion pairs $[C^{z+} S A^{z-}]^o$ or $[C^{z+} S S A^{z-}]^o$. Ionic equilibria in solution are not limited to ion-pair formation. Depending on the permittivity of the solvent and the short-range interactions of the solutes chemists assume bilateral triple-ion formation $[C^+ A^- C^+]^+$ and $[A^- C^+ A^-]^-$; unilateral triple-ion formation occurs when only the positively or negatively charged triple ion is formed.

Ionogenes, such as an acid AH, which form their ions in solution by chemical reactions of the electrolyte and the solvent S produce ion pairs in an ionization step prior to dissociation

$$AH + S \overset{k_I}{\rightleftharpoons} [SH^+ A^-]^o \overset{k_D}{\rightleftharpoons} SH^+ + A^- \quad (30)$$

Fig. 3: Argand diagrams showing solvent (left semicircleof each curve) and ion-aggregate relaxation (right demi-circle) regions of aqueous solutions.

a: MgSO₄   b: CdCl₂

(1) pure water; (2) 0.363 M solution;   (1) 0.298 M solution,

(3) 1.10 M solution   (2) 1.45 M solution

Ion aggregate responsible for the relaxation process:

SSIP: $[Mg^{2+}(H_2O)SO_4^{2-}]^o$ CIP: $[Cd^{2+} Cl^-]^+$

Table 1: Association and rate constants of ion-pair formation from dielectric relaxation data (K_A, k_1, k_2) and literature values $K_A^{Lit.}$ at 25°C.

solvent	electrolyte	IP	K_A $\mathrm{mol\,dm^{-3}}$	K_A^{Lit}	$k_1 \cdot 10^{-9}$ $\mathrm{dm^3\,mol^{-1}\,s^{-1}}$	$k_2 \cdot 10^{-9}$ $\mathrm{s^{-1}}$
water	Na₂SO₄	SSIP	18±1	4.5[1]	6.5± 0.5	0.37 ± 0.03
	MgSO₄	SSIP	164±25	174[2]	1.8± 0.1	0.011± 0.001
	CdCl₂	CIP	105±65	85[3]	8.3± 1.8	0.097± 0.022
	CdSO₄	SSIP	270±90	245[4]	2.3± 1.4	0.009± 0.002
methanol	Bu₄NClO₄	CIP	44±17	47.1[5]	a)	
acetonitrile	LiBr	CIP	148±2	155—193*	b)	
	NaI	CIP	17±6	3.8—24*	8± 1	0.4± 0.1
	NaClO₄	CIP	31±3	15—27*	10.7± 0.4	0.44± 0.04
	Bu₄NBr	CIP	17±1	17—22*	8.0± 0.3	0.35± 0.03
DMF	NaClO₄	SSIP	1.9±1.3	3.2±0.7[6]	4.7± 0.2	1.5± 0.3
DMSO	LiNCS	CIP	≈ 3	≈ 1[7]	b)	

* re-analysis of various conductance data from the literature; a) determination of τ^{kin} not possible; b) $\tau^{kin} \gg \tau^{or}$; [1] R.M.Izatt, D.Eatough, J.J.Christensen, and C.H.Bartholomew, J. Chem. Soc. A (1969) 47; [2] H.-J.Wittmann, PhD-Thesis, Regensburg 1985; [3] P.J.Reilly and R.H.Stokes, Aust. J. Chem. 23 (1970) 1397; [4] J.Barthel, R.Buchner, and H.-J.Wittmann, Z. Phys. Chem. NF 139 (1984) 23; [5] J.Barthel, M.Krell, L.Iberl, and F.Feuerlein, J. Electroanal. Chem. Interfacial Electrochem. 214 (1986) 485; [6] B.S.Krumgalz and J.Barthel, Z. Phys. Chem. NF 142 (1984) 167; [7] J.B.Gill and P.Longdon, personal communication.

As far as ion aggregates have dipoles, such as the neutral ion pairs $[C^+ A^-]^o$, $[C^+ S A^-]^o$, $[C^{2+} S A^{z-}]^o$ etc. or charge bearing ion pairs $[C^{2+} A^-]^+$, $[C^{2+} S A^-]^+$, $[C^+ A^{2-}]^-$ etc., and their life time is not shorter than the signal time imposed by the electromagnetic wave they are orientable in the electric field and reveal their proper relaxation processes, see figs. 3.

The dispersion amplitude of ion-pair relaxation permits the calculation of the ion-pair concentration $c_{IP} = 10^{-3} N_A \rho_{IP}$, see eq. (23), and hence the ion-pair association constant; the dipole moment μ_{IP}, its polarizability α_{IP} and reaction field factor f_{IP} can be estimated from appropriate ion-pair models and reveal whether the ion pair is a contact ion pair (CIP) or solvent-separated ion pair (SSIP) [13].

Generally, the concentration dependence of the ion-pair relaxation time is incompatible with theoretical expectations leading to the conclusion that the rotational diffusion process of the ion pair is superimposed by a kinetic mode [12][13][45][46]. The kinetic process shown by eq. (29a) yields a variation of μ_{IP} resulting from the changing mutual distance of cation and anion during the ion-pair formation and dissociation process. This change is measurable at frequencies where the reciprocal kinetic relaxation time $(\tau^{kin})^{-1}$ is of the order of the signal frequency. As an example, the symmetrical electrolyte $C^{z+} A^{z-}$ produces the kinetic relaxation time

$[k_2 + 2k_1(c - c_{IP})]^{-1}$ [47], and the superimposition of the orientational and kinetic relaxation times yields the observable relaxation time

$$(\tau_{IP}^{obs})^{-1} = (\tau_{IP}^{or})^{-1} + k_2 + 2k_1(c - c_{IP}); \quad K_{ass} = \frac{k_1}{k_2} \qquad (31\text{a,b})$$

Data analysis according to eqs. (31) yields the quantities k_1, k_2 and τ_{IP}^{or}, K_{ass} being known from the dispersion amplitude. The case of charged ion pairs of unsymmetrical electrolytes can be treated in a similar way. Examples for various types of ion aggregation are given in table 1.

Table 1 contains the association constants K_A obtained by extrapolation to infinite dilution of the electrolyte, $\lim_{c \to o} K_{ass} = K_A$, which may be compared to association constants from calorimetric or conductance measurements quoted in the column K_A^{Lit}.

3. The Chemical Models of Electrolyte Solutions

3.1 Theoretical background

The knowledge on the structure of electrolyte solutions revealed by high frequency permittivity measurements, but also from IR, NMR and Raman spectroscopy, scattering experiments and the almost unlimited information from thermodynamic and transport investigations on electrolyte solutions have improved classical electrolyte theory and have led to efficient models for the calculation of electrolyte solution properties, such as the chemical model for dilute electrolyte solutions or MSA (mean spherical approach) and HNC (hypernetted chain) models for the more concentrated solutions.

Chemical models are Hamiltonian models at the level of McMillan-Mayer (MM) or Born-Oppenheimer (BO) approximations.

At BO level the solvent is taken into account by the interactions of a solvent molecule both with solutes and other solvent molecules. At MM level the solvent is averaged out and the properties of the solution are discussed in terms of ion-ion interactions in a homogeneous medium representing the solvent. The Debye-Hückel theory is the lowest level of MM approximations. A detailed analysis of the actual state of the situation concerning BO and MM level models is given in ref. [48]. In this paper only the MM level will be discussed.

Friedman and Dale [49] showed that the price which must be paid for the transformation of the grand partition function into an effective grand partition function only of ion-ion interactions is the non-additivity of the solvent averaged potential U_N of the direct pair interactions between ions

$$U_N(\vec{r}_1...\vec{r}_N) = \sum_{i,j} u_{ij}(\vec{r}_1, \vec{r}_2) + \sum_{i,j,k} u_{ijk}(\vec{r}_1, \vec{r}_2, \vec{r}_3) + ... \qquad (32)$$

In eq. (32) u_{ij} is the pair potential of particles i and j, u_{ijk} is the triplet potential of i, j, k etc. As a first approximation, the right hand side can be truncated after

the first term, neglecting all non-pairwise interactions. This approximation entails that the corresponding theories are restricted to dilute or moderately concentrated solutions. The common strategy is to produce a tractable relation between the direct interaction potentials u_{ij} and the potential of mean force W_{ij} which, in turn, reflects the influence of all other ions in the solution on the interaction between the ions i and j under consideration. In general this relation is given by the expression

$$-\vec{grad}\, W_{ij}(\vec{r}_1, \vec{r}_2) = \frac{\int ... \int (-\vec{grad}\, U_N) \exp(-\beta U_N) d\vec{r}_3...d\vec{r}_N}{\int ... \int \exp(-\beta U_N) d\vec{r}_3...d\vec{r}_N}; \quad \beta = \frac{1}{kT} \qquad (33\text{a,b})$$

Spherical symmetry permits to write $u_{ij}(r), r = |\vec{r}_1 - \vec{r}_2|$, instead of $u_{ij}(\vec{r}_1, \vec{r}_2)$. The use of eqs. (32) and (33) yields the ion-ion pair-correlation functions $g_{ij}(r)$

$$g_{ij}(r) = \exp[-\beta W_{ij}(r)] \qquad (34)$$

Pair-correlation functions $g_{ij}(r)$ are related to the so-called pair-distribution functions $f_{ij}(r)$ by the relationship

$$f_{ij}(r) = \rho_i \rho_j g_{ij}(r) = f_{ji}(r) \qquad (35)$$

Distribution functions $f_{ij}(r)$ indicate the probability of finding two ions i and j in the solution at distance r, irrespective of the position of all other ions and the velocity of all ions.

3.2 The chemical model of dilute solutions

In order to obtain equations for the properties of electrolyte solutions which are valid beyond the Debye-Hückel limiting law at low to moderate concentrations a MM model must be used that takes into account both long-range and short-range forces around the ions. For this purpose the chemical model of electrolyte solutions subdivides the space around an ion into three regions [50 to 53]

(i) $r \leq a$, a being the minimum distance of two oppositely charged ions which is assumed to be the sum of effective cation and anion radii, $a = a_+ + a_-$.

(ii) $a \leq r \leq R$, within which a paired state of oppositely charged ions, the ion pair $[C^{z+}A^{z-}]^o$, suppresses long-range interactions with other ions in the solution. In dilute solutions the occupation of this region by ions of equal sign can usually be neglected.

(iii) $r \leq R$, the range of long-range ion-ion interactions.

The distance parameters a and R are fixed by chemical evidence [53].

Table 2 shows the mean force potentials for a dilute solution of a symmetrical electrolyte $C^{z+}A^{z-}$; W_{+-}^* is a step potential which equals zero for $r \leq a$ and $r \geq R$ characterizing the short-range forces superimposed to the long-range forces W_{ij}^{el} around the ions

$$W_{ij}(r) = W_{ij}^{el}(r) + W_{ij}^* \qquad (36)$$

Table 2: Mean force potentials $W_{ij}(r)$ of ion-ion interaction in dilute solutions of symmetrical electrolytes $C^{z+}A^{z-}$ [53]
$\kappa^2 = \frac{N_A e^2}{\varepsilon_o \varepsilon kT} \sum_j 10^3 \alpha c_j z_j^2$; c_j : molality of the electrolyte, α: degree of dissociation

Region	Mean force potential
$r \leq a$	∞
$a \leq r \leq R$	$\dfrac{e^2 z_i z_j}{4\pi\varepsilon_o\varepsilon} \cdot \dfrac{1}{r} - \dfrac{e^2 z_i z_j}{4\pi\varepsilon_o\varepsilon} \dfrac{\kappa}{1+\kappa R} + W_{ij}^*$
$r \geq R$	$\dfrac{e^2 z_i z_j}{4\pi\varepsilon_o\varepsilon} \cdot \dfrac{1}{r} \cdot \dfrac{\exp[\kappa(R-r)]}{1+\kappa R}$

The chemical model permits an unambiguous inclusion of the ion-pair concept into the theory [52]

$$K_{ass} = 4000\pi N_A \int_a^R r^2 \exp[-\frac{W_{ij}(r)}{kt}]dr \qquad (37)$$

For the mean force potential $W_{ij}(r)$ in the region $a \leq r \leq R$ see table 2.

The association constant K_{ass} can be subdivided into the thermodynamic equilibrium constant K_A and the activity coefficient $y_\pm'$ of the freely moving ions in the solution

$$K_A = 4\pi N_A \int_a^R r^2 \exp[-\frac{2q_{+-}}{r} - \frac{W_{+-}^*}{kT}]; \quad y_\pm' = \exp[\frac{\kappa q_{+-}}{1+\kappa R}] \qquad (38a,b)$$

where q_{+-} is the Bjerrum parameter

$$q_{+-} = \frac{e^2 z_+ z_-}{8\pi\varepsilon_o\varepsilon kT} \qquad (39)$$

From eqs. (38) Bjerrum's association constant [54] and its appropriate activity coefficient are obtained when setting $R = -q_{+-}$ and $W_{+-}^* = 0$. The assumption that $a = R$ in eqs. (38) yields the activity coefficient of the Debye-Hückel theory for a completely dissociated electrolyte ($K_A = 0$); $a = 0$ leads to the activity coefficient of the limiting law.

The mean activity coefficient $y_\pm$ of the electrolyte compound is given in the framework of the chemical model for completely dissociated symmetrical electrolytes ($\alpha = 1$) or partially associated symmetrical electrolytes ($\alpha < 1$) by the relation

$$y_\pm = \alpha y_\pm' \qquad (40a)$$

The degree of ion-pair dissociation is calculable from eq. (38a) where

$$K_A = \frac{1-\alpha}{\alpha^2 c} \cdot \frac{1}{y_\pm'^2} \qquad (40b)$$

The knowledge of assciation constant and activity coefficient permits the calculation of the thermodynamic properties of electrolyte solutions on the base of chemical potentials μ_E of the electrolyte compound

$$\mu_E(p,T) = \mu_E^\infty(p,T) + 2RT lnc + 2RT lny_\pm \qquad (41)$$

The reciprocal process is more commonly used: the calculation of association constants and/or activity coefficients from measured thermodynamic properties.

Transport equations such as the conductance equation

$$\Lambda = \alpha[\Lambda^\infty - S(\alpha c)^{1/2} + E(\alpha c)ln(\alpha c) + J_1(R)\alpha c + J_2(R)(\alpha c)^{3/2}] \qquad (42)$$

are also based on chemical models, for details see ref. [55]. In eq. (42) Λ and Λ^∞ are the equivalent conductances at concentrations c and at infinite dilution of the electrolyte compound; α is given by eq. (40b). The coefficients S and E are independent of the distance parameters R; J_1 and J_2 depend on R. All parameters, except S depend on the model underlying a particular conductance theory. The reader is referred to refs. [55 to 58] where the coefficients are compiled.

The completely dissociated electrolyte follows eq. (42) when setting $R = a$ and $\alpha = 1$. The Onsager limiting law of conductance ($a = 0$) is given by the expression [59]

$$\Lambda = \Lambda^\infty - S\sqrt{c} \qquad (43)$$

Equations are given in the literature also for single ion conductances and transference numbers [60][61] at the level of eq. (42). Triple-ion formation is treated at the level of eq. (43). This is not a real drawback. Triple-ion formation is always accompanied by very strong ion-pair formation permitting the application of limiting laws up to moderate electrolyte concentrations since the concentration of free ions remains within the validity range of these approximations.

It is an important and well-proved feature of the chemical model that association constants of a given electrolyte solution determined from any thermodynamic or transport property are equal and may be used to calculate every other property and its temperature or pressure dependence [53]. The equality of association constants obtained by various thermodynamic properties and those from high frequency permittivity measurements was stressed in table 1. Valuable information on ion association is also obtained from spectroscopic methods [62 to 69], showing that the study of dilute solutions is as actual as ever for the provision of information on electrolyte solutions.

Other important fields of application of chemical model calculations for dilute solutions are the study of mixed solvent systems [70], the determination of specific solvation, e.g. investigations on ion-solvent complexes [71 to 73], the study of the

role of water traces in non-aqueous solutions [74], or the study of bilateral and unilateral triple-ion formation [75 to 77]. Such investigations gain increasing importance by the need for information on technically used, sometimes rather complex organic solvent systems [53]. For transport processes and coupled transport processes in electrolyte solutions see ref. [78].

4. Integral Equation Methods

4.1 Theoretical background

Integral equation methods for the determination of thermodynamic properties are exemplified here only for HNC methods [79 to 81] at McMillan-Mayer level. For MSA (mean spherical approach) [82], PY (Perkus-Yevik) [83], and combined methods [84 to 86] the reader is referred to the literature; the extension of integral equation methods to time-dependent quantities is given in refs. [87 to 89], extensions to the Born-Oppenheimer level can be found in ref. [90].

Various statistical thermodynamic equations provide the link between pair-correlation functions $g_{ij}(r)$ and direct pair potentials $u_{ij}(r)$ on the one hand and thermodynamic properties on the other hand.

Examples will be given in the following text on osmotic coefficients ϕ based on the virial equation [91]

$$\phi - 1 = -\frac{\beta}{6\rho}\sum \rho_i \rho_j \int r \frac{\partial u_{ij}(r)}{\partial r} g_{ij}(r) 4\pi r^2 dr, \quad \rho = \sum \rho_i \qquad (44a,b)$$

Integral equations, in turn, provide the link between direct interaction potentials $u_{ij}(r)$ and radial distribution function $g_{ij}(r)$

$$g_{ij}(r) = \exp[-\beta u_{ij}(r) + \Upsilon_{ij}(r)] \qquad (45)$$

The function $\Upsilon_{ij}(r)$ is the difference between the direct pair potential and the mean force potential, $\Upsilon_{ij}(r) = \beta[u_{ij}(r) - W_{ij}(r)]$, cf. eq. (34).

For integral equations the appropriate representation of the pair-correlation functions is given by the expression

$$g_{12}(r) = \frac{V^2}{Q_N} \int \prod_{i<j} \exp[-\beta u_{ij}(r)] d\vec{r}_3 ... d\vec{r}_N; \quad Q_N = \int \exp[-\beta U_N] d\vec{r}_1 ... d\vec{r}_N$$

$$(46a,b)$$

Q_N is the configurational integral of classical statistical mechanics. The use of Mayer F-functions, $F_{ij}(r) = \exp[-\beta u_{ij}(r)] - 1$, permits the development of $g_{12}(r)$ in the form

$$g_{12}(r) = \frac{V^2}{Q_N} \int [1 + \sum_{pairs} F_{ij} + \sum_{triplets} (F_{ij}F_{jk} + F_{ij}F_{jk}F_{ki}) + ...] d\vec{r}_3 ... d\vec{r}_N \qquad (47)$$

Graph theory [91] offers the possibility to rearrange the infinite sums and products of integrals and to reduce them. The remaining integrals can be arranged in few well defined classes. In calculations at MM-level $u_{ij}(r)$ is replaced by the mean force potential W_{ij}^∞ at infininte dilution ($\kappa = 0$). The result of such operations yields

$$g_{ij}(r) = \exp[-\beta W_{ij}^\infty(r) + \Upsilon_{ij}(r)] \qquad (48a)$$

$$\Upsilon_{ij}(r) = S_{ij}(r) + B_{ij}(r); \quad W_{ij}^\infty(r) = \frac{2q_{ij}kT}{r} + W_{ij}^*(r); \quad q_{ij} = \frac{e^2 z_i z_j}{8\pi\varepsilon_o \varepsilon kT} \qquad (48b,c,d)$$

where $S_{ij}(r)$ is the sum of all series graphs and $B_{ij}(r)$ is the sum of all bridge graphs of the cluster development. Graph theroy shows that $g_{ij}(r)$ and $S_{ij}(r)$ are related via the total correlation functions, $h_{ij}(r) = g_{ij}(r) - 1$, and the direct correlation functions c_{ij}

$$S_{ij}(r) = h_{ij}(r) - c_{ij}(r); \quad h_{ij}(r) = c_{ij}(r) + \sum_k \rho_k \int c_{ik}(r) h_{kj}(r) d\vec{r}_k \qquad (49a,b)$$

where ρ_k is the density of particles k. Eq. (49b) is the Ornstein-Zernicke equation. The sum of bridge graphs is generally neglected in integral equation methods, $\Upsilon_{ij}(r) = S_{ij}(r)$. In eqs. (48a,b) $S_{ij}(r)$ can be considered as an additional concentration-dependent term to the direct interaction potential $c_{ij}(r)$ taking into account the indirect interactions between two particles i and j via all other solute particles.

This outline of the integral equation theory shows that the calculation of the pair-correlation functions $g_{ij}(r)$ via eq. (44a) meets only the short-range potential $W_{ij}^*(r)$ as unknown quantities. Vice versa, from measured thermodynamic properties the short-range interaction potentials $W_{ij}^*(r)$ may be determined as the adaption parameters and then yield information on the interactions in the solution.

4.2 HNC methods and results

The neglection of the bridge functions in eq. (48a) yields the HNC equation

$$g_{ij}(r) = \exp[-\beta W_{ij}^\infty(r) + S_{ij}(r)] \qquad (50)$$

which can be solved numerically together with eqs. (49) in an iteration process. Convergence problems due to Coulomb interactions must be overcome with the help of appropriate changes of the initial HNC algorithm [92].

The simplest way to introduce short-range potentials into the theory is the choice of a step potentials for $++, +-$ and $--$ interactions [79][81], thus extending the concept of the chemical model at low concentrations, section 3.2, to higher concentrations. The comparison, given in fig. 4, of the non-Coulombian step potentials ($\Delta G_{+-}^* = N_A W_{+-}^*; W_{+-}^*$ according to eq. (36)) obtained from low concentration chemical

model ($lcCM$) calculations and HNC calculations using step potentials for the short-range interactions (HNC-SP) shows a strong linear correlation revealing the same structural effects [93].
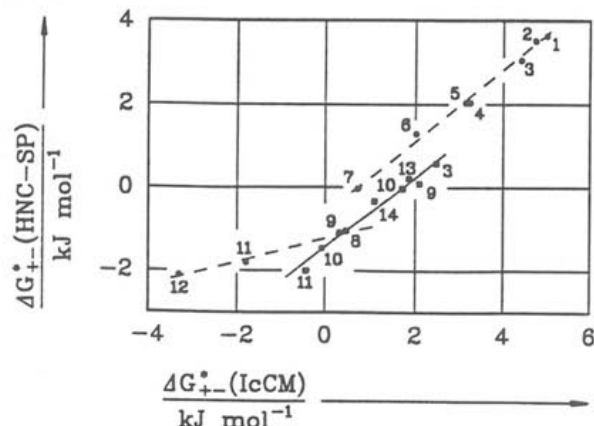

Fig. 4: Correlation of the non-Coulombian interaction energies ΔG^{*}_{+-} from lcCM and HNC-SP calculations carried out at equal cut-off distances R_{+-} for every salt [93]. broken lines: methanol solutions; full line: acetonitrile solutions; salts (points: methanol solutions, squares: acetonitrile solutions) 1: NaCl; 2: NaBr; 3: NaI; 4: NaClO$_4$; 5: KI; 6: RbI; 7: CsI; 8: Et$_4$NBr; 9: Bu$_4$NBr; 10: Pent$_4$NBr; 11: Bu$_4$NI; 12: Bu$_4$NClO$_4$; 13: Bu$_4$NCl; 14: Pr$_4$NBr

$R_{+-} = a_+ + a_- + s; a_+, a_-$: cation and anion radii, s: length of a solvent molecule.

A more elaborated approach is due to Friedman and Rasaiah who subdivide the short-range potential into three parts [94][95]

$$W^{*}_{ij} = COR_{ij}(r) + GUR_{ij}(r) + CAV_{ij}(r) \qquad (51)$$

$COR_{ij}(r)$ is a soft repulsive potential, proportional to $(a_{ij}/r)^n$ where the ion contact parameter a_{ij} and the exponent n (typical is n = 9) are the potential parameters; the Guerney sphere contribution, $GUR_{ij}(r) = A_{ij}V_{mu}/V_s$, results from the overlap of the solvation spheres when two ions have approached to distances less than the thickness of their solvation shells. V_s is the molar volume of the pure solvent, V_{mu} is the overlap volume. The Helmholtz energies A_{ij} needed for the exclusion of solvent from the solvation shells are the adjustable parameters of the theory. $CAV_{ij}(r)$, proportional to r^{-4}, reflects the mutual ion polarization; this effect is rather small. Step potentials for W^{*}_{ij} and continuous potentials according to eq. (51) yield equally good reproductions of the thermodynamic properties of electrolyte solutions. Fig. 5 shows the pair-correlation functions $g_{++}(r), g_{+-}(r)$ and $g_{--}(r)$ of various 0.1 M tetraalkylammonium salt solutions in acetonitrile obtained with the help of HNC calculations with continuous short-range potentials as given by eq.(51) [96]. Brownian dynamics simulations at MM-level using the structure factors

from small-angle neutron scattering [97] verify these pair-correlation functions, thus showing by an independent method that the neglect of the bridge functions in HNC calculations is justifiable [48]. Examples for the successful reproduction of osmotic coefficients of non-aqueous electrolyte solutions with the help of HNC calculations up to high concentrations and critical remarks on the method can be found in refs. [86][93][96][98 to 101]. The use of solution permittivities from MW-measurements for the calculation of mean force potentials instead of the permittivities of the pure solvents is discussed in ref. [86].
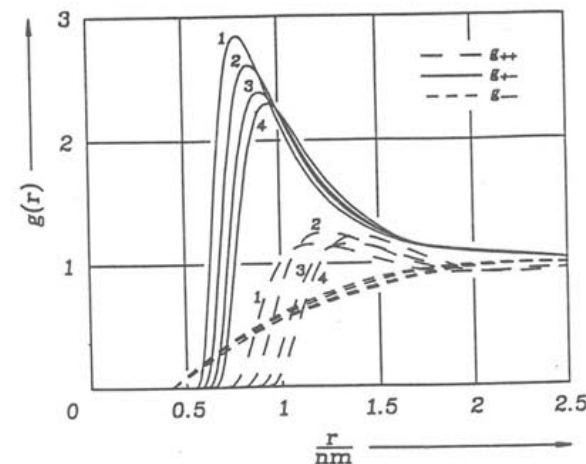

Fig. 5: Pair-correlation functions $g_{++}(r), g_{+-}(r)$ and $g_{--}(r)$ from HNC calculations for 0.1 M acetonitrile solutions of several tetraalkylammonium bromides at 25° C: 1: Et$_4$NBr; 2: Pr$_4$NBr; 3: n-Bu$_4$NBr; 5: n-Pent$_4$NBr [96].

5. Concluding remarks

It is a feature of Hamiltonian models at McMillan-Mayer level that several models reproduce a property of an electrolyte solution equally well. Theory cannot provide a criterion for the best model. However, the best model out of a variety of models should permit the reproduction of various solution properties with the help of a unique set of model parameters which have chemical evidence. This strategy for the choice of 'best' models was repeatedly used for electrolyte solutions at low to moderate concentrations with the help of chemical models, recent results are also available for HNC methods where model parameters were simultaneously fitted; it is also the basic concept of the knowledge-based electrolyte data base ELDAR combining a comprehensive literature and data collection with a method bank containing the moduls of about 40 equations of electrolyte solution and solvent properties needed for the construction of property diagrams for scientific and technical research. Valuable information on model parameters is also obtained from FIR, IR and NMR measurements, computer simulations and scattering experiments. These methods are gaining increasing interest for the provision of fundamental research and technology with data on the structure and properties of electrolyte solutions.

References

[1] J. Barthel, H. Popp, G. Schmeer in: J. Gasteiger (ed.): Software Development in Chemistry, Vol. 2, Springer, Berlin 1988, 127

[2] J. Barthel, H. Popp, G. Schmeer in: J. Gasteiger (ed.): Software Development in Chemistry, Vol. 4, Springer, Berlin 1990, 101

[3] J. Barthel, H. Popp, J. Chem. Inf. Comput. Sci., in press

[4] H.-J. Gores, J. Barthel, Naturwissenschaften 70 (1983) 495

[5] J. Powles, J. Chem. Phys. 21 (1953) 633; S. H. Glarum, J. Chem. Phys. 33 (1960) 1371

[6] J. L. Dote, D. Kivelson, R. N. Schwartz, J. Phys. Chem. 85 (1981) 2169

[7] C. F. J. Böttcher, P. Bordewijk: Theory of Electric Polarization (2nd ed.), Vol. 2, Elsevier, Amsterdam 1978

[8] H.-J. Wittmann, Thesis Dr. rer. nat., Regensburg 1985

[9] J. Barthel, R. Buchner, H. Steger, Wiss. Z. Tech. Hochsch. „Carl Schorlemmer" Leuna-Merseburg 31 (1989) 409

[10] J. Barthel, R. Buchner, K. Bachhuber. H. Hetzenauer, M. Kleebauer, H. Ortmaier, Pure Appl. Chem. 62 (1990) 2287

[11] J. Barthel, K. Bachhuber, R. Buchner, H. Hetzenauer, Chem. Phys. Lett. 165 (1990) 369

[12] J. Barthel, K. Bachhuber, R. Buchner, J.B. Gill, M. Kleebauer, Chem. Phys. Lett. 167 (1990) 62

[13] J. Barthel, R. Buchner, Pure Appl. Chem., in press

[14] E. A. S. Cavell, P. C. Knight, M. A. Seikh, J. Chem. Soc. Faraday Trans. I 67 (1971) 2225

[15] S. K. Garg, C. P. Smyth, J. Phys. Chem. 69 (1965) 1294

[16] E. Noreland, B. Gestblom, S. Sjöblom, J. Solution Chem. 18 (1989) 303

[17] M. W. Sagal, J. Chem. Phys. 36 (1962) 2437

[18] R. Groot Wassink and P. Bordewijk, Adv. Mol. Relax. Interact. Processes 13 (1978) 299

[19] B. Gestblom, J. Sjöblom, Act. Chem. Scand. A38 (1984) 47; 575

[20] S. Mashimo, S. Kuwabara, S. Yagihara, K. Higasi, J. Chem. Phys. 90 (1989) 3292

[21] U. Kaatze, C. Neumann, R. Pottel, J. Solution Chem. 16 (1987) 191

[22] U. Kaatze, R. Pottel, P. Schmidt, J. Phys. Chem. 92 (1988) 3669

[23] D. F. Calef, P. G. Wolynes, J. Chem. Phys. 78 (1983) 4145

[24] J. T. Hynes, J. Phys. Chem. 90 (1986) 3701

[25] M. Marconelli, E. W. Castner Jr., B. Bagchi, G. R. Fleming, Faraday Discuss. Chem. Soc. 85 (1988) 199

[26] M. J. Weaver, E. G. McManis, W. Jarzeba, P. F. Barbara, J. Phys. Chem. 94 (1990) 1715

[27] G. Grampp, A. Kapturkiewicz, W. Jaenicke, Ber. Bunsenges. Phys. Chem. 94 (1990) 439

[28] J. T. Hupp, M. J. Weaver, J. Electroanal. Chem. 152 (1983) 1

[29] J. Barthel in: P. Huyskens, Th. Huyskens-Zeegers, W.A.P. Luck (eds.), Intermolecular Forces - An Introduction to Modern Methods and Results. Chapter XVIII, Springer, Berlin 1991

[30] J. Barthel, K. Bachhuber, R. Buchner in: M. Moreau, P. Turq (eds.), Chemical Reactivity in Liquids - Fundamental Aspects, Plenum, New York 1988, 55

[31] J. Barthel, R. Buchner, Pure Appl. Chem. 58 (1986) 1077

[32] U. Kaatze, D. Adolph, D. Gottlob, R. Pottel, Ber. Bunsenges. Phys. Chem. 84 (1980) 1198

[33] U. Kaatze, Z. Phys. Chem. N.F. 135 (1983) 51

[34] K. Giese, U. Kaatze, R. Pottel, J. Phys. Chem. 74 (1970) 3718

[35] J.-C. Lestrade, J.-P. Badiali, H. Cachet in: M. Davies (ed.), Dielectric and Related Molecular Properties, Vol. 2, The Chemical Society, London 1975, 106

[36] J.P. Badiali, H. Cachet, J.-C. Lestrade, J. Chim. Phys. Phys.-Chim. Biol. 64 (1967) 1350

[37] J. B. Hubbard, L. Onsager, J. Chem. Phys. 67 (1977) 4850

[38] J. B. Hubbard, J. Chem. Phys. 68 (1978) 1649

[39] K. Ibuki, M. Nakahara, J. Chem. Phys. 84 (1986) 2776

[40] K. Ibuki, M. Nakahara, J. Phys. Chem. 91 (1987) 1864; 4411; 4414

[41] Y. M. Kessler, R. S. Kumeev, I. I. Vaisman, R. B. Lyalina, R. H. Bratishko, Ber. Bunsenges. Phys. Chem. 93 (1989) 770

[42] B. U. Felderhof, Mol. Phys. 51 (1984) 801

[43] J. B. Hubbard, P. Colonomos, P. G. Wolynes, J. Chem. Phys. 71 (1979) 2652

[44] J. Barthel, Pure Appl. Chem. 57 (1985) 355

[45] H. Strehlow, W. Knoche: Fundamentals of Chemical Relaxation, Verlag Chemie, Weinheim 1977

[46] P. Turq, L. Orcil, M. Chemla, J. Barthel, Ber. Bunsenges. Phys. Chem. 85 (1981) 535

[47] M. Eigen, K. Tamm, Z. Electrochem. 66 (1962) 93

[48] W. Kunz, P. Turq, J. Barthel, Ann. Phys. (Paris), in press

[49] H.L.Friedman and W.D.T.Dale in: B.J. Berne (ed.): Modern Theoretical Chemistry, Vol.5.: Statistical Mechanics, Part A: Equilibrium Techniques, Plenum, New York 1977, 85

[50] J.C.Rasaiah and H.L.Friedman, J. Phys. Chem. 72 (1968) 3352

[51] J.C.Rasaiah, J. Chem. Phys. 52 (1970) 704

[52] J. Barthel, Ber. Bunsenges. Phys. Chem. 83 (1979) 252

[53] J. Barthel, H.-J. Gores, G. Schmeer, R. Wachter in F.L. Boschke: Top. Curr. Chem. 111 (1983) 33

[54] N. Bjerrum, Kgl. danske Videnskab. Selskab., math.-fysiske Medd. 7, No.9 (1926) 1

[55] J.-C. Justice in: B. E. Conway, J.O'M. Bockris, E. Yeager (eds.), Comprehensive Treatise of Electrochemistry, Vol. 5, Plenum, New York 1983, 223

[56] J. Barthel: Ionen in nichtwäßrigen Lösungen, Dr.Dietrich Steinkopf, Darmstadt 1976

[57] J. Barthel, J.-C. Justice, R. Wachter, Z. Phys. Chem. N. F. 84 (1973) 100

[58] J. Barthel, R. Buchner, H.-J. Wittmann, Z. Phys. Chem. N.F. 139 (1984) 23

[59] L. Onsager, Phys. Z. 27 (1926) 388; 28 (1927) 277

[60] J. Perié, M. Perié, J.-C. Justice, J. Solution Chem. 9 (1980) 395

[61] J.-C. Justice, J. Perié, M. Perié, J. Solution Chem. 9 (1980) 583

[62] J. B. Gill, Pure Appl. Chem. 53 (1981) 1365

[63] P. Gans, J. B. Gill, M. Griffin and P.C. Cahill, J. Chem. Soc. Dalton Trans. (1981) 968

[64] G. J. Janz, M. A. Müller, J. Solution Chem. 4 (1975) 285

[65] J. Rannou, M. Chabanel, J. Chim. Phys. Phys.-Chim. Biol. 77 (1980) 201

[66] D. Paoli, M. Luçon, M. Chabanel, Spectrochim. Acta 35A (1979) 593

[67] W. F. Edgell, S. Hedge, A. Barbetta, J. Am. Chem. Soc. 100 (1978) 1406

[68] W. F. Edgell, S. Chanjamsri, J. Am. Chem. Soc. 102 (1980) 147

[69] M. Krell, M. C. R. Symons, J. Barthel, J. Chem. Soc. Faraday Trans. I 83 (1987) 3419

[70] A. K. Covington, T. Dickinson (eds.): Physical Chemistry of Organic Solvent Systems, Plenum, New York 1973

[71] E. K. Ralph III, W. R. Gilkerson, J. Am. Chem. Soc. 86 (1984) 4783

[72] J. B. Ezell, W. R. Gilkerson, J. Phys. Chem. 72 (1968) 144; H. W. Aitken, W. R. Gilkerson, J. Am. Chem. Soc. 95 (1973) 8551

[73] J. Macau, L. Lamberts, P. Huyskens, Bull. Soc. Chim. Fr. (1971) 2387

[74] J. Barthel, R. Buchner, H.-J. Gores in: DECHEMA Monographien, Bd. 124, DECHEMA, Frankfurt (in press)

[75] R. M. Fuoss, C. A. Kraus, J. Am. Chem. Soc. 55 (1933) 2387

[76] J. Barthel, R. Gerber, H.-J. Gores, Ber. Bunsenges. Phys. Chem. 88 (1984) 616

[77] C.B. Wooster, J. Am. Chem. Soc. 59 (1937) 377

[78] P. Turq, M. Chemla, J. Barthel: Transport, Relaxation and Kinetic Processes of Electrolyte Solutions, Springer, Berlin (in press)

[79] J. C. Rasaiah, H. L. Friedman, J. Phys. Chem. 72 (1968) 3352

[80] J. C. Rasaiah, H. L. Friedman, J. Chem. Phys. 50 (1969) 3965

[81] J. C. Rasaiah, J. Chem. Phys. 52 (1970) 704

[82] L. Blum in: H. Eyring, D. Henderson (eds.): Theoretical Chemistry: Advances and Perspectives, Vol. 5, Academic Press, New York 1980, 1

[83] J. K. Percus, G. J. Yevick, Phys. Rev. 110 (1958) 1

[84] F. J. Rogers, D. A. Young, Phys. Rev. A30 (1984) 999

[85] G. Zerah, J. P. Hansen, J. Chem. Phys. 84 (1986) 2336

[86] W. Kunz, J. Barthel, J. Solution Chem. 19 (1990) 339

[87] A. R. Altenberger, H. L. Friedman, J. Chem. Phys. 78 (1983) 4162

[88] E. C. Zhong, H. L. Friedman, J. Phys. Chem. 92 (1988) 1685

[89] M. D. Wood, H. L. Friedman, Z. Phys. Chem. N.F. 155 (1987) 121

[90] P. G. Kusalik, G. N. Patey, J. Chem. Phys. 88 (1988) 7715; 89 (1988) 5843; 7478

[91] H. L. Friedman: A Course in Statistical Mechanics, Prentice Hall, Englewood Cliffs, New Jersey 1985

[92] A. R. Allnatt, Mol. Phys. 8 (1964) 533

[93] J. Barthel, W. Kunz, G. Lauermann, R. Neueder, Ber. Bunsenges. Phys. Chem. 92 (1988) 1372

[94] H. L. Friedman, P. S. Ramanathan, J. Phys. Chem. 74 (1970) 3756

[95] P. S. Ramanathan, H. L. Friedman, J. Chem. Phys. 54 (1971) 1086

[96] J. Barthel, W. Kunz, J. Solution Chem. 17 (1988) 399

[97] W. Kunz, P. Calmettes, P. Turq, J. Chem. Phys. 92 (1990) 2367

[98] G. Lauermann, W. Kunz, J. Barthel, J. Solution Chem. 16 (1987) 871

[99] R. Bacquet, P. J. Rossky, J. Chem. Phys. 79 (1983) 1419

[100] P. J. Rossky, J. B. Dudowicz, B. L. Tembe, H. L. Friedman, J. Chem. Phys. 73 (1980) 3372

[101] J. B. Valleau, L. K. Cohen, D. N. Card, J. Chem. Phys. 72 (1980) 5942